Deformation and Flow of a Two-Dimensional Foam under Continuous Shear

G. Debrégeas,* H. Tabuteau, and J.-M di Meglio†

Institut Charles Sadron, CNRS UPR 022, 6 rue Boussingault, 67083 Strasbourg Cedex, France

(Received 21 March 2001; published 9 October 2001)

We investigate the flow properties of a 2D foam (a confined monolayer of jammed bubbles) submitted to a continuous shear in a Couette geometry. A strong localization of the flow at the moving inner wall is evidenced. Moreover, velocity fluctuations measurements reveal self-similar dynamical structures consisting of clusters of bubbles moving coherently. A stochastic model is proposed where bubbles rearrangements are activated by local stress fluctuations produced by the shearing wheel. This model gives a complete description of our observations and is also consistent with available data on granular shear bands.

DOI: 10.1103/PhysRevLett.87.178305 PACS numbers: 82.70.Rr, 83.80.Iz

Disordered systems, such as foams, concentrated emulsions, slurries, or granular materials, exhibit rheological properties that cannot be understood within the scope of standard solid or liquid mechanics [1–3]. For such systems, thermal energies are orders of magnitude lower than the typical energy required to relax the structural arrangements of their components; under small forces, the material remains trapped in a metastable configuration and exhibits a solidlike behavior. However, when submitted to a large enough stress, it can be driven through a series of new metastable configurations, giving rise to a macroscopic flow. But the resulting flow field may still differ a lot from what would be expected for a molecular liquid.

Dry sand slowly flowing down an hour glass provides a simple example of such abnormal flow behaviors: the flow splits into a pluglike central region and a strongly sheared thin layer at the wall — a few particles wide — where most of the dissipative process occurs [4]. This spontaneous localization of the strain in narrow regions (the so-called shear bands) can be observed in many other situations such as shear, surface or convective flows for instance [5–8]. Shear banding actually controls most of the practical situations encountered in soil mechanics and industrial handling of grains, and is also relevant to pyroclastic flows in geology (for a review on granular matter, see [9]). This question has recently received a lot of attention from physicists, both theoretically and experimentally [10,11], but a clear picture has not emerged yet.

By contrast, the possibility of shear banding in foams has been mostly ignored in the literature, and numerical or theoretical studies usually assume shear flows in foams to be uniform [2,12]. The assumption that shear banding is unique to granular matter can be misleading because it suggests that some peculiar aspects of granular flows, such as solid friction, particle rotation, or dilatancy, are essential.

In this Letter, we report the formation of shear bands in aqueous foams. We believe that foams may shed light on the dynamics of granular systems by evidencing the minimal set of ingredients needed to get shear banding. To that extent, foams constitute a much simpler model than granular systems since the basic bubble/bubble interactions which control the mechanical properties of the material are well known: elastic (stored) energy is related to an increase of the total interfacial area when the bubbles are distorted, whereas dissipated energy is associated with neighbors swapping events (T_1 processes) inducing flows in the liquid films and vertices (for a review on foams, see [13]).

In order to probe the microdynamics of the foam, one needs to track the trajectory of each bubble. Since 3D foams are inherently diffusive to light, we used a 2D model foam — a confined monolayer of bubbles — submitted to a continuous slow shear in a wide-gap Couette geometry. The setup was composed of an inner shearing wheel and an outer ring (of respective radius $R_0 = 71$ mm and $R_1 = 122$ mm) confined between two transparent plates separated by a 2 mm gap. To produce the foam, the cell was first held vertically and partially filled with a known volume of soap/water solution. Bubbles were formed by blowing nitrogen gas through two small injection holes at different flow rates until the resulting foam reached the top of the cell. Once set horizontally, the foam rapidly attained a uniform wetness characterized by its liquid fraction $0.01 < \phi < 0.3$ (Fig. 1). This foaming procedure was chosen because it produces bidisperse disordered foams and therefore eliminates crystallization. The mean diameters within each of the two populations of bubbles were of the order of 2 and 2.7 mm, with a mean deviation of 0.2 mm. These bubbles were large enough compared to the gap height so that they would not overlap. To define a bubble scale, we measured the mean distance d between first neighbors in the foam. We kept $2.1 < d < 2.5$ mm so that the gap between the wheel and the ring could accommodate from 20 to 25 rows of bubbles. The distance d was evaluated several times during the experiment and found to be almost constant. Coarsening would eventually lead to a growth of the biggest bubbles at the expense of the smallest ones but over a longer time. We also checked the absence of shear induced size segregation that might have occurred during the experiment.

Shearing was induced by rotating the inner wheel at constant velocity V_{wheel} using a stepper motor. To avoid

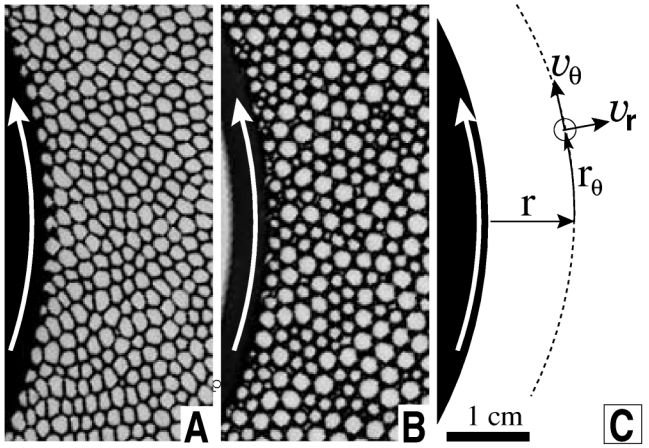

FIG. 1. Close-up frames of dry and wet 2D foams under continuous shear. The shearing wheel appears in black. Arrows indicate the inner wheel direction of rotation. (**A**) A dry bidisperse foam ($\phi = 0.05$), showing deformed polygonal cells. (**B**) A wet bidisperse foam ($\phi = 0.20$). The bubbles are circular and undeformed. (**C**) System of coordinates used to analyze the flow field.

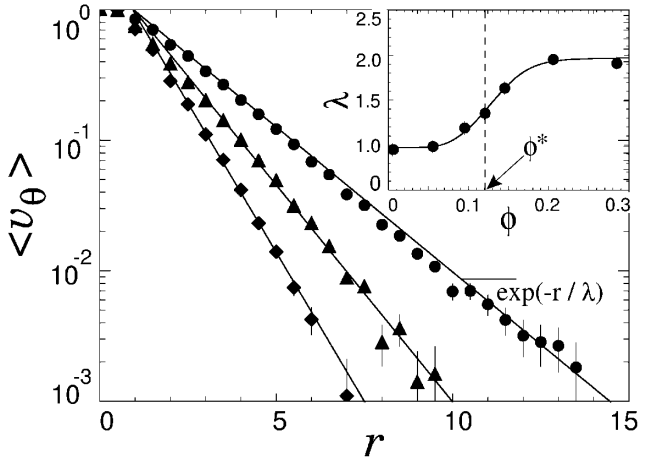

FIG. 2. Average tangential velocity profiles for different liquid fraction (◆: $\phi = 0.05$; ▲: $\phi = 0.12$; •: $\phi = 0.20$), showing exponential decays with a width $\lambda(\phi)$. The small plateau for $0 < r < 1$ corresponds to the first row of bubbles being attached to the shearing wheel. Inset: Dependence of λ on liquid fractions ϕ (the line is just a guide for the eyes). Two plateaus can be distinguished on either side of $\phi^* \simeq 0.12$, which separate polygonal and circular bubbles regimes.

slippage at the wheel and the ring, their sides were tooth shaped so that the first and last rows of bubbles would remain irreversibly attached to the walls. To eliminate transient effects, we ran the experiment a full round before taking data. The motion of 1000 to 1500 bubbles was then recorded using a CCD digital camera positioned over the setup. In a typical experiment, 3000 images were taken corresponding to a total displacement of $600d$ of the wheel edge. The apparent centers of mass of the bubbles were subsequently tracked by image analysis (IDL software). To reduce the effect of the viscous friction between the bubbles and the confining plates, we restricted our study to quasistatic flows. We focused on average velocity measurements as a probe of shear rate dependence: we found that in the range $0 < V_{\text{wheel}} < 0.7$ mm $\cdot$ s^{-1}, the velocity profiles were similar apart from an overall scale factor. All experiments were performed in the quasistatic regime at $V_{\text{wheel}} = 0.25$ mm $\cdot$ s^{-1}. In the following, all velocities and distances are normalized by V_{wheel} and d, respectively. We note $\omega_0 = V_{\text{wheel}}/d$ the characteristic frequency of the shear.

Figure 2(A) shows the decay of the average tangential velocity $\langle v_\theta(r) \rangle$ with the distance r to the shearing wheel for different liquid fractions ϕ [see Fig. 1(C) for variables definition]. Averaging was performed over the tangential coordinate r_θ and time t, yielding smooth and reproducible profiles, although the instantaneous flow is strongly intermittent. The reduced velocity is found to approach 1 at $r \to 0$ confirming the absence of slip at the edge of the wheel. At larger r, the profiles exhibit an exponential decay

$$\langle v_\theta(r) \rangle \sim \exp(-r/\lambda), \tag{1}$$

with a width λ depending on ϕ. The curve λ versus ϕ, presented in Fig. 2 (inset), shows two plateaus at low and high volume fraction. The transition between these two regimes occurs around $\phi^* = 0.12$, which qualitatively marks the limit between dry foams with polygonal bubbles for $\phi < \phi^*$ and wet foams with circular bubbles for $\phi > \phi^*$. In both cases, the rapid decay of the mean velocity over a few bubble diameters establishes the existence of shear banding in foams. The exponential shape of the velocity profile, observed in all experiments, appears as a robust feature which was also observed in comparable experiments performed on 2D granular materials [4,5,14].

Beyond these time averaged profiles, our setup allows measurements of the short time scale fluctuations of the bubbles velocities. A mere observation of the video sequences reveals brief oscillations of clusters of bubbles of various radial extension, rotating together as rigid bodies as shown in Fig. 3. These dynamical structures are ephemeral and disappear after the wheel edge has moved by roughly one bubble diameter (this was checked by measuring time correlations of the velocity which decay to 0 in a time of order $1/\omega_0$). To quantitatively probe these coherent moves, we studied the spatial correlations of the instantaneous velocity field. We focused on the radial component v_r which has a zero time average and therefore gives a better signal to noise ratio (qualitatively, similar results were found when using $v_\theta - \langle v_\theta \rangle$ instead of v_r). Figure 4(A) shows the correlation function $g_r(\Delta r_\theta) = \langle v_r(r, r_\theta) \cdot v_r(r, r_\theta + \Delta r_\theta) \rangle / \langle v_r^2(r) \rangle$ for different values of r from 1 to 10, at a volume fraction $\phi = 0.20$. Regardless of r, g_r decreases with Δr_θ from 1 to a negative value then slowly relaxes to 0. The length $\xi(r)$

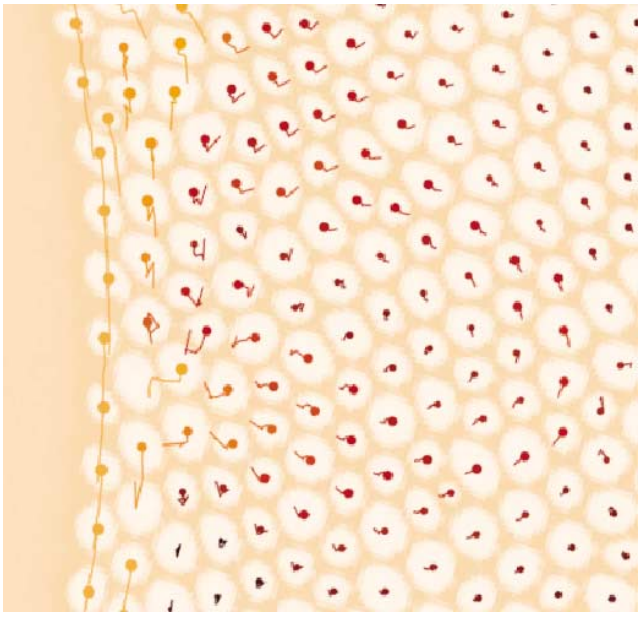

FIG. 3 (color). Video frame of the foam with the position of the bubbles centers and their trajectories over the last 20 sec. This time period corresponds to a total displacement of one bubble diameter for the first row (or equivalently for the inner disc edge). The dots size and lines color reflect the total distance traveled by the bubbles revealing a large rotating cluster.

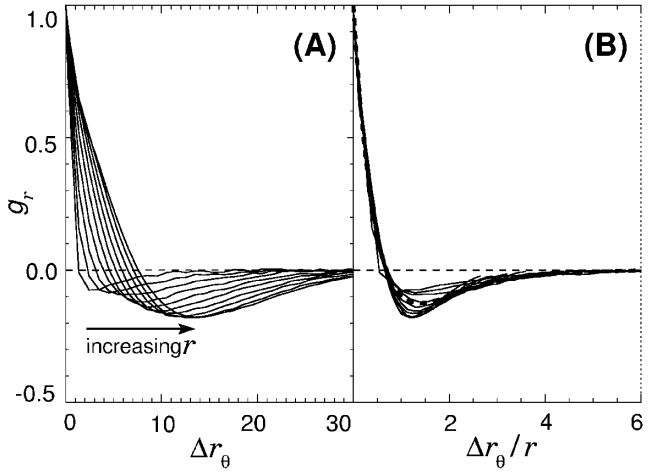

FIG. 4. (A): Spatial correlations of the radial velocity for different radial distances r from 1 to 10 ($\phi = 0.15$). (B): All correlations can be collapsed on a single curve when plotted versus the tangential distance rescaled by r. To fit this master curve, we assume that the radial velocity $v_r(r, r_\theta)$ at different r comes from the rotation of clusters of mean lateral extension $\xi(r)$ proportional to r [$\xi(r) = \alpha r$]. The radial velocity field within a cluster of size μ is idealized by a two step function ($v_r = \epsilon v_0$ for $-\mu < r_\theta < 0$ and $v_r = -\epsilon v_0$ for $0 < r_\theta < \mu$ with $\epsilon = \pm 1$). We postulate a statistical distribution of μ around $\xi(r)$ by assuming that the fraction of clusters of size larger than μ is $\exp(-\frac{\mu}{\xi(r)})$. The resulting correlation function (dotted line) then reads $g_r(\Delta r_\theta) = (1 - \frac{\Delta r_\theta}{\alpha r}) \exp(-\frac{\Delta r_\theta}{\alpha r})$.

for which g_r reaches 0 defines a typical correlation length of the velocity field at distance r. In Fig. 4(B), r_θ has been rescaled by r. All curves then collapse on a single one, which demonstrates a linear increase of $\xi(r)$ with the radial distance r: $\xi(r) = \alpha r$. Motivated by the observation of oscillating clusters, we modeled the flow field as a superimposition of rotating blocks of bubbles of various sizes (see figure caption for details) which allowed us to obtain a good fit of the master curve [Fig. 4(B)]. Similar results were obtained at all volume fractions, and the coefficient α was found to decrease with ϕ.

It should be noted that the velocity field which yields the measured correlation functions mainly corresponds to reversible moves and thus probes the elastic deformation of the foam rather than the plastic flow. The quantity $\sqrt{\langle v_r^2 \rangle}/\langle v_\theta \rangle$ provides a good estimate of the ratio of reversible to irreversible moves. This quantity is larger than 1 beyond the first attached row of bubbles, and gets larger than 10 beyond the fifth row. The correlation measurements thus reveal that the instantaneous *stress* field is spatially correlated.

This peculiar characteristic of the foam deformation field can actually be understood under the scope of linear elasticity, by modeling the foam as an isotropic elastic medium. In the following, we neglect the radial geometry of the experiment (the wheel radius being much larger than the shear band width) and thus assume parallel shear. During the initial loading, a uniform mean shear stress $\overline{\sigma}$ builds up in the material. In the steady state, this uniform stress persists in average but is locally modulated by a fluctuating stress field $\Delta\sigma(t)$ of mean value 0 associated with the continuous rubbing of the wheel teeth. At each location $(r = 0, r_\theta = i)$ on the wheel edge, the foam is indeed submitted to a localized perturbative stress $\Delta\sigma_i(t)$ of variance $s_0 = \langle \Delta\sigma_0^2 \rangle$ varying at a frequency ω_0 which elastically propagates into the material. These multiple noise sources add up to produce a stress fluctuation at a position (r, r_θ) of amplitude (see, for instance, [15]):

$$\Delta\sigma_r(r_\theta, t) \simeq \sum_i \frac{\Delta\sigma_i(t)}{\sqrt{r^2 + (r_\theta - i)^2}} . \qquad (2)$$

Assuming the noise sources to be uncorrelated [$\langle \Delta\sigma_i(t) \times \Delta\sigma_j(t) \rangle = 0$ for $i \neq j$], the resulting stress coherence length, at distance r, takes the form $\xi(r) = \alpha r$, in agreement with our experimental findings. We interpret the different observed values for α as a signature of the anisotropy of the foam due to its initial loading. This is consistent with the observation of large values of α for the driest foams where the largest uniform deformation is first produced. From Eq. (2), we are also able to compute the variance of the fluctuating stress $\Delta\sigma_r(t)$ as

$$\langle \Delta\sigma_r^2 \rangle = s(r) \sim \frac{s_0}{\alpha r} . \qquad (3)$$

We now relate the fluctuating stress field $\Delta\sigma_r(t)$ to the average flow profile by taking into account the foam plasticity. Our approach mostly follows a model proposed by Pouliquen and Gutfraind [4] based on Eyring's activated

process theory [16] to describe chute flows of granular materials. In the present description, the variance of the local stress fluctuation $s(r)$ plays the role of a temperature allowing plastic flow to occur. The moving boundary acts as a "hot wall," exciting internal deformation modes in the form of self-similar rotating clusters. When the fluctuating stress overcomes a certain yield value σ_y, the structure plastically yields. The yielding rate in the material by unit of time and space thus writes $\omega = \omega_0 P(\sigma > \sigma_y)$, where $P(\sigma)$ is the density probability of stress. The stress at a distance r is a sum of $\sim r$ random variables [see Eq. (2)] so that $P[\sigma(r)]$ is a Gaussian distribution centered on $\overline{\sigma}$ of variance $s(r)$. Using Eq. (3), the yielding rate at a distance r reads

$$\omega(r) = \omega_0 P[\sigma(r) > \sigma_y] = \omega_0 \left(1 - \mathrm{erf}\sqrt{\frac{r}{\lambda}}\right), \quad (4)$$

with

$$\lambda = \frac{1}{\alpha} \frac{2s_0}{(\sigma_y - \overline{\sigma})^2}. \quad (5)$$

Each failure increments the average velocity gradient by 1 in reduced unit, so that the constitutive equation for the flow writes $\frac{\partial \langle v_\theta(r) \rangle}{\partial r} \sim -\omega(r)/\omega_0$ with the boundary conditions $\langle v_\theta(0) \rangle = 1$ and $\langle v_\theta(\infty) \rangle = 0$. A very good approximate function to the integral of $\omega(r)$ is given by a pure exponential so that $\langle v_\theta(r) \rangle \simeq \exp(-r/\lambda)$ in good agreement with our experimental findings.

In conclusion, we have observed shear banding in dry and wet 2D foams under continuous slow shear and we have probed the associated elastic deformations of the foam, characterized by brief, collective oscillations of self-similar blocks of bubbles. We have developed a stochastic model which relates the plastic flow to the stress fluctuations. The main characteristics of the flow (rapid decay of the average velocity over a few bubbles, large velocity fluctuations) are very similar to what is commonly observed in granular systems, suggesting that the proposed mechanism could remain valid for granular systems. As already mentioned, the predicted exponential velocity decay has been observed in various 2D granular shear bands [4,5,7]. Moreover, the velocity profile in 3D has been shown to obey a Gaussian decay in the limit of disordered and nonspherical grains [6]. This functional form for the velocity profile immediately follows from the modification of Eq. (3) in 3D which then writes $s(r) \sim \frac{s_0}{\alpha^2 r^2}$ yielding a Gaussian decay for $\langle v_\theta \rangle$.

We are grateful to D. Mueth for helping us with the image analysis. We wish to thank A. Kabla, S. Roux, and C. Josserand for stimulating discussions.

*Corresponding author.
Electronic address: debregea@ics.u-strasbg.fr.
†Also at Université Louis Pasteur and Institut Universitaire de France.

[1] P. Sollich, F. Lequeux, P. Hebraud, and M. E. Cates, Phys. Rev. Lett. **78**, 2020 (1997).
[2] S. A. Langer and A. J. Liu, Europhys. Lett. **49**, 68 (2000).
[3] A. Liu and S. Nagel, Nature (London) **396**, 21 (1998).
[4] O. Pouliquien and R. Gutfraind, Phys. Rev. E **53**, 552 (1996).
[5] D. Howell, R. P. Behringer, and C. Veje, Phys. Rev. Lett. **82**, 5241 (1999).
[6] D. Mueth, G. Debrégeas, G. Karczmar, P. J. Eng, S. Nagel, and H. Jaeger, Nature (London) **406**, 385 (2000).
[7] T. S. Komatsu, S. Inagaki, N. Nakagawa, and S. Nasuno, Phys. Rev. Lett. **86**, 1757 (2001).
[8] J. B. Knight, E. E. Ehrichs, V. Y. Kuperman, J. K. Flint, H. M. Jaeger, and S. R. Nagel, Phys. Rev. E **54**, 5726 (1996).
[9] P.-G. de Gennes, Rev. Mod. Phys. **71**, S374 (1999).
[10] J. Torok, S. Krishnamarthy, J. Kertesz, and S. Roux, Phys. Rev. Lett. **84**, 3851 (2000).
[11] G. Debrégeas and C. Josserand, Europhys. Lett. **52**, 137 (2000).
[12] D. J. Durian, Phys. Rev. Lett. **75**, 4780 (1995).
[13] D. Weaire and S. Hutzler, *The Physics of Foams* (Clarendon Press, Oxford, 1999).
[14] W. Losert, L. Bocquet, T. C. Lubensky, and J. P. Gollub, Phys. Rev. Lett. **85**, 1428 (2000).
[15] K. L. Johnson, *Contact Mechanics* (Cambridge University Press, Cambridge, United Kingdom, 1985).
[16] K. Glasstone, J. Laider, and H. Eyring, *The Theory of Rate Processes* (McGraw-Hill, New York, 1941).